



Intensification of drying processes due to optimal operations



S.J. Kowalski, A. Rybicki, K. Rajewska*

Poznań University of Technology, Institute of Technology and Chemical Engineering, pl. Marii Skłodowskiej-Curie 2, 60-965 Poznań, Poland

ARTICLE INFO

Article history:

Received 14 June 2014

Received in revised form 16 September 2014

Accepted 3 October 2014

Available online 22 October 2014

Keywords:

Optimization

Convective drying

Energy consumption

Numerical simulations

ABSTRACT

Based on the drying theory developed earlier by the authors, this paper presents some results of computerized simulation of convective drying of a solid material, leading to optimal drying conditions; thus, offering minimum energy consumption and high product quality obtained at a maximum yet permissible drying rate. The thermo-hydro-mechanical model of drying is used to describe the kinetics of drying and to analyze drying-induced stresses which are responsible for damage of dried products. The effective stress defined on the basis of the energetic criterion is related to the admissible stress; thus, constituting the strength criterion for a given material. Three different numerical examples of effective drying are presented based on a sample of finite dimensions of a kaolin-clay cylinder subjected to convective drying.

© 2014 Elsevier B.V. All rights reserved.

1. Introduction

The drying rate, energy consumption and quality of dried products constitute the three most important criteria which are taken into account when assessing drying effectiveness [1–6]. This paper shows the possibilities of how to construct effective drying processes on the basis of the drying theory that was elaborated earlier by the authors. The numerical tests concern suitable control of the drying air temperature and humidity as well as the dosage of energy needed to obtain a high drying rate, minimum energy consumption, and good product quality [7–9]. Optimization of drying parameters is conducted through programming the computer memory in such a way that the drying-induced stresses are close to the admissible stresses but never exceed them. In this way the material does not suffer damage and the drying rate is high.

Based on the above-mentioned mathematical model of drying, three examples of numerically simulated drying processes and their optimal control with respect to the above-mentioned criteria are presented. The first example was carried out at constant and possibly severe drying conditions but without material damage. In the second example the stresses were controlled during the whole process and allowed to be close to the admissible stresses but never exceeded them. In the third tested process the main optimization criterion was minimum energy consumption. In this case the method of the genetic algorithm is used for optimal operation with drying conditions. A chain of directives consisting

of zero and unity is used to code the optimal work of the fan and the heater in the drying set-up [7,10]. The numerically simulated optimal drying processes of convective drying regard to cylindrical samples made of kaolin clay, which reflect properties characteristic for ceramic-like materials.

2. Preliminaries

The sample in the form of finite dimensions of a kaolin-clay cylinder that was used for the numerical tests is presented in Fig. 1, [11–15].

The rate of drying depends on the rate of moisture transport from the material interior to the surface, from where it is removed to the surroundings in the form of vapor. In common convective drying the process can be accelerated through an increase in the temperature and decrease in the humidity of the drying medium (air) as well as in an increase of the drying medium (air) flow around the drying body. As for the latter, in order to describe the effect of agent speed on the drying rate in numerical analysis based on the drying model it would be necessary to relate the coefficients of heat α_T and mass α_m transfer (see Eqs. (8)a and b) with the speed of the drying medium flow. This way of increasing the drying rate is not considered here; however, we are aware that the speed of the drying agent flow affects the above-mentioned coefficients and the drying rate.

Here we will consider an increase in the drying rate provoked by an increase in the moisture capacity in the drying agent through an increase in its temperature ϑ_a and reduction in absolute humidity Y_a , or relative humidity ϕ_a . Table 1 and Fig. 2 show the effect of two different quantities of ϑ_a and Y_a on the drying rate and on the

* Corresponding author.

E-mail address: kinga.rajewska@put.poznan.pl (K. Rajewska).

Nomenclature

A	elastic bulk modulus [MPa]
a_T	thermal diffusivity [m^2/s]
c_v	specific heat [J/kg K]
c_T	coefficient of thermodiffusion [m^2/sK]
c_X	coefficient of diffusion [m^2/s^2]
H	cylinder height [m]
l	latent heat of evaporation [J/kg]
M	elastic shear modulus [MPa]
p	pressure [Pa]
r, R	cylinder radius [m]
\mathfrak{R}	gas constant [J/kg K]
t	time [s]
T	temperature [K]
$u(u_r, u_z)$	displacement vector [m]
Y_a	absolute air humidity [kg water vapor/kg dry air]
z	spatial Cartesian coordinates [m]
X	dry basis moisture content [$kg_{water}/kg_{drybody}$]

Greek symbols

α_m	coefficient of convective vapor exchange [$kg\ s/m^4$]
α_T	coefficient of convective heat exchange [$W/m^2\ K$]
μ^v	chemical potential of vapor [J/kg]
$\kappa^{(T)}$	coefficient of thermal expansion [1/K]
$\kappa^{(X)}$	coefficient of humid expansion [1]
ε_{ij}	strain tensor [1]
ε	volumetric strain [1]
σ_{ij}	stress tensor [Pa]
ρ^s	mass density of dry body [kg/m^3]
ω	phase transition coefficient [$kg\ s/m^5$]
$\vartheta = T - T_r$	temperature with respect to reference state [$^{\circ}C$]
$\theta = X - X_r$	moisture content with respect to reference state [1]
Λ_X	mass transport coefficient of α -constituent [$kg\ s/m^3$]
Λ_T	coefficient of thermal conductivity [$W/m\ K$]

magnitude of effective stresses generated in the material during drying [7,10].

All of the numerical results presented in Fig. 2 were obtained for the same material constants and initial conditions: $\theta_{0av} = 0.4$ and $\vartheta_0 = 20^{\circ}C$. As can be noticed in Fig. 2, faster removal of moisture (Fig. 2a, curve II) caused greater non-uniformity in the distribution of moisture content (see Figs. 14 and 15), which led to the generation of greater effective stresses (Fig. 2b, curve II). Thus, the possibility of material damage appears when more intensive drying is involved. This can be stated by comparing the drying-induced effective stresses with the admissible stress representing the strength of the drying material (Fig. 2b). As is shown in Fig. 2b, material strength depends on moisture content, which varies in time (Fig. 2a), and material strength increases in the course of drying as the material becomes more dry.

The curves in Fig. 2b show the time evolution of the maximal effective and admissible stresses which arose in the corner of the cylindrical sample (Fig. 1) (point (R, H)) for slow (I) and fast (II) drying processes. As follows from the presented curves, possible material damage can take place during process II, where the effective stress overcomes the admissible stress.

On the other hand, in an analysis of the plots presenting the time evolution of maximal effective stresses for process I a large reserve of material strength can be noticed. Such a strength reserve allows to significantly accelerate the drying rate through suitable

operation of the drying parameters. However, operating with the parameters is not as simple because material behavior during drying is nonlinear, and it would be difficult to foresee precisely and in advance how the stresses would be induced after the drying agent parameters had been modified. Therefore, designing an efficient drying process which would assure a high drying rate and simultaneously would not cause material damage requires a number of numerical experiments, called the optimization procedure.

3. Modeling

The numerical drying tests presented in this paper are based on the thermo-hydro-mechanical model of drying as developed in Kowalski [16–18], which is here adopted to determine the stresses and the radial and longitudinal displacements u_r and u_z , in the cylindrical sample (Fig. 1)

$$M\nabla^2 u_r + \frac{\partial}{\partial r}[(M+A)\varepsilon - y^{(T)}\vartheta - y^{(X)}\theta] = M\frac{u_r}{r^2} \quad (1a)$$

$$M\nabla^2 u_z + \frac{\partial}{\partial z}[(M+A)\varepsilon - y^{(T)}\vartheta - y^{(X)}\theta] = 0 \text{ with } \nabla^2 = \frac{\partial^2}{\partial r^2} + \frac{1}{r}\frac{\partial}{\partial r} + \frac{\partial^2}{\partial z^2} \quad (1b)$$

where ∇^2 denotes the axially symmetric Laplace operator, $\vartheta = T - T_r$ and $\theta = X - X_r$ denote the temperature and moisture content referred to as a reference state, and $X [-]$ expresses the mass of moisture referred to as the mass of dry body. The thermo- and hydro-mechanical parameters $\gamma^{(T)} = (2M + 3A)\kappa^{(T)}$ and $\gamma^{(X)} = (2M + 3A)\kappa^{(X)}$ which appear in these equations are related to the respective coefficients of thermal- $\kappa^{(T)}$ and hygro- $\kappa^{(X)}$ expansion; M and A denote the shear and bulk elastic moduli of the material, and ε denotes the volumetric strain expressed as:

$$\varepsilon = \frac{\partial u_r}{\partial r} + \frac{u_r}{r} + \frac{\partial u_z}{\partial z} \quad (2)$$

The mechanical boundary conditions assume zero radial σ_{rr} and longitudinal σ_{zz} stresses on the external surfaces, and zero radial u_r and longitudinal u_z displacements on the axis and in the cylinder center, that is (Fig. 1),

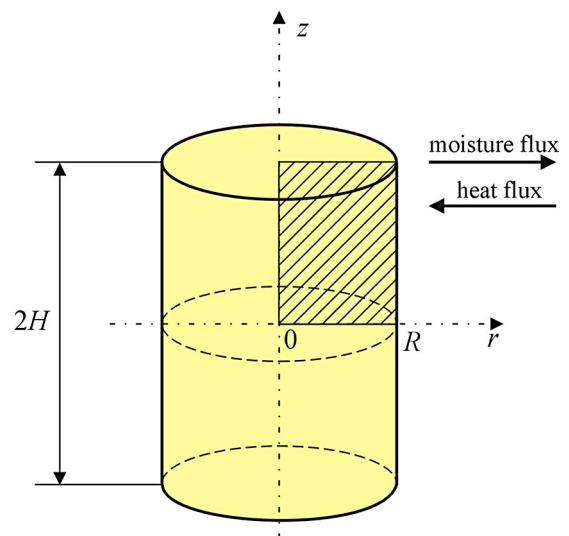


Fig. 1. Cylindrical sample used in the numerical tests.

Download English Version:

<https://daneshyari.com/en/article/688140>

Download Persian Version:

<https://daneshyari.com/article/688140>

[Daneshyari.com](https://daneshyari.com)